

## Excitation of the two-phonon giant dipole resonance in $^{238}\text{U}$ studied via inclusive measurements of neutron-removal cross sections

T. Aumann<sup>a</sup>, K. Sümmerer<sup>b</sup>, C.A. Bertulani<sup>c</sup>, J.V. Kratz<sup>a</sup> and the FRS-collaboration<sup>1,d</sup>

<sup>a</sup>Inst. f. Kernchemie, Univ. Mainz, D-55099 Mainz, Germany

<sup>b</sup>GSI Darmstadt, P.O. Box 110552, D-64289 Darmstadt, Germany

<sup>c</sup>Inst. de Fisica, Univ. Fed. Rio de Janeiro, C.Postal 68528, Rio de Janeiro, Brazil

<sup>d</sup>GSI and TH Darmstadt, Univ. Giessen, CEN Bordeaux, Univ. Warsaw, IPN Orsay

As part of a comprehensive study of uranium fragmentation at relativistic energies at the GSI projectile fragment separator, FRS, inclusive neutron-removal cross sections have been measured for several  $xn$  channels at projectile energies of 600 and 950 A MeV. The electromagnetic cross sections agree surprisingly well with a semiclassical calculation based on measured photonuclear cross sections and do not require an extra enhancement of the two-phonon giant dipole excitation as concluded from similar measurements with  $^{197}\text{Au}$ .

### 1. INTRODUCTION

The study of multi-phonon giant resonances in nuclei is a topic of current interest both for experimentalists and theorists [2,3]. One of the puzzles concerning the Coulomb excitation of the double giant dipole resonance (DGDR) is the higher than calculated cross section observed for some nuclei [4–7]. Though detailed information on the resonance parameters of multi-phonon giant resonances can only be obtained from exclusive measurements, inclusive measurements of few-neutron-removal cross sections can provide information on the cross sections of such resonances. Measurements of  $1n$  to  $3n$  cross sections of target-like  $^{197}\text{Au}$  fragments have shown that the  $2n$  and in particular the  $3n$  cross sections are very sensitive to the strength of the DGDR [6,8].

In this paper we present  $xn$  cross sections for  $^{238}\text{U}$  projectiles with energies of 600 and 950 A MeV impinging on  $^{27}\text{Al}$ ,  $^{nat}\text{Cu}$ , and  $^{208}\text{Pb}$  targets, measured at the GSI projectile fragment separator FRS [9]. The data are complementary to results from experiments studying target-like fission of  $^{238}\text{U}$  induced by  $^{208}\text{Pb}$  beams [10] and projectile-like fission of  $^{238}\text{U}$  [11,12] in the energy range between 100 and 1000 A MeV.

We will show below that all our measured  $xn$  cross sections are in agreement with a semiclassical calculation in the harmonic approach, in contrast to the study of neutron-removal from  $^{197}\text{Au}$ , where we had to invoke an increased DGDR excitation probability to reproduce the experimental cross sections [6,8].

## 2. EXPERIMENTAL METHOD AND RESULTS

Beams of  $^{238}\text{U}$  accelerated to energies of 600 and 950 A MeV by the GSI heavy-ion synchrotron SIS were directed onto targets of  $^{27}\text{Al}$ ,  $^{nat}\text{Cu}$ , and  $^{208}\text{Pb}$ . The neutron removal products  $^{233-237}\text{U}$  were separated spatially and identified with respect to nuclear charge and mass,  $Z$  and  $A$ , with the GSI projectile fragment separator FRS [9] by measuring their magnetic rigidity behind the target and a second time after passing an aluminum degrader. From the number of observed fragments behind the FRS, production cross sections were obtained, as described in detail in Ref. [13]. In Fig. 1 the resulting  $1n - 3n$  cross sections are shown for both beam energies.

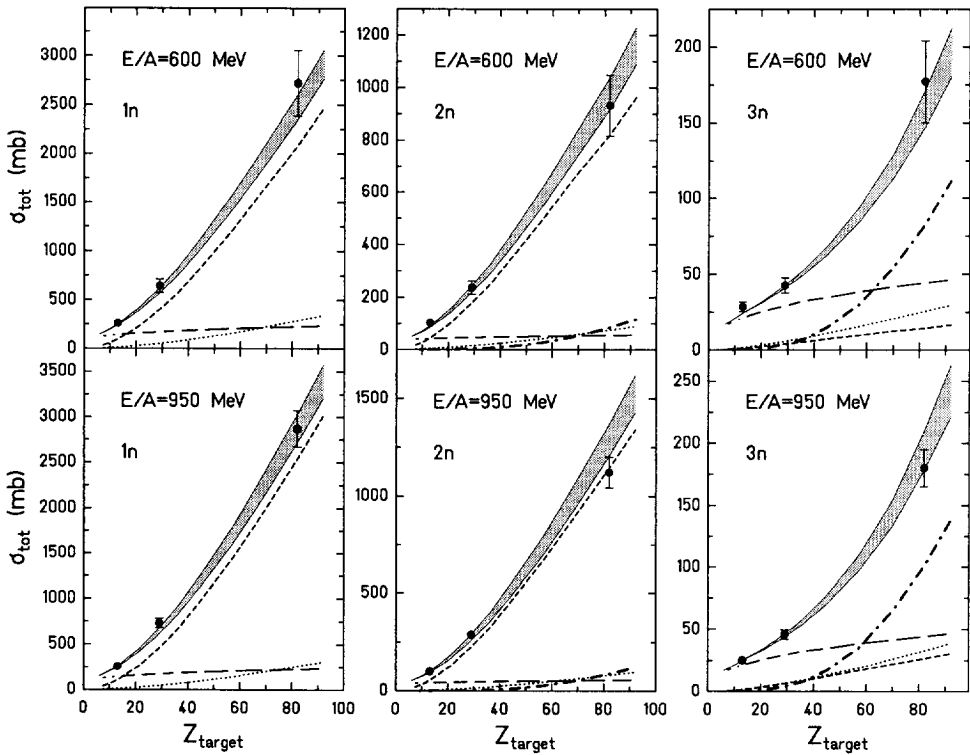


Figure 1. Cross sections for the formation of the  $1n$ - to  $3n$ -removal products from  $^{238}\text{U}$  projectiles at about 600 A MeV (upper part) and 950 A MeV (lower part) incident on targets with  $Z_{\text{target}}$ . The full curves delineating the hatched areas denote our theoretical calculations using two different experimental GDR parameter sets [14,15]. They represent the sum of the nuclear contribution (long-dashed curve), and the electromagnetic contributions due to excitation of the GDR (short-dashed curve), GQR (dotted curve), and DGDR (dot-dashed curve).

To disentangle nuclear and electromagnetic contributions, the nuclear cross sections for low  $Z$ , where the ED part is less important, were determined from experimental data. The  $xn$  cross sections for heavier reaction partners were then obtained assuming the same  $A^{1/3}$ -dependence as in Ref. [6]. The results for the nuclear contributions are indicated in Fig. 1 by the long-dashed curves. It is obvious that for the Pb target the  $1n$  and  $2n$  channels have a nuclear contribution that is of similar size as the experimental error of the data and can therefore be neglected in our discussion. The  $3n$  channel has a 25% contribution from nuclear processes.

### 3. SEMI-CLASSICAL CALCULATIONS

To interpret the experimental data, we will compare the ED part of the cross sections with a semiclassical calculation using empirical parametrizations of the giant dipole (GDR) and giant quadrupole (GQR) resonances. DGDR excitations are taken into account assuming a harmonic vibration [16,17]. Apart from the giant-resonance strength functions, which can be taken from experiment, such a calculation has a more or less free parameter, the minimum impact parameter  $b_{min}$ . It is assumed that below  $b_{min}$  the interaction is exclusively nuclear, whereas above pure Coulomb interactions occur ('sharp-cutoff' approximation). We have investigated the proper choice of  $b_{min}$  in Ref. [13] for the system 1 A GeV  $Z_{projectile} + {}^{197}\text{Au}$ . In Fig. 2 we compare experimental  $1n$  and  $3n$  ED cross

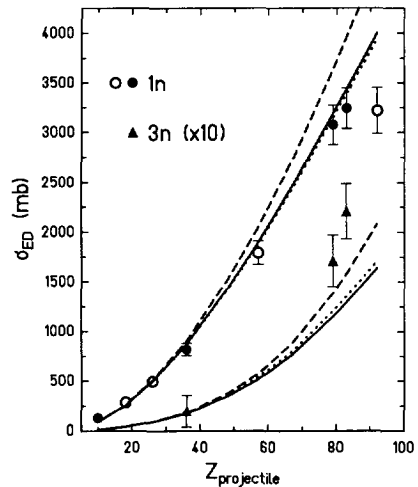


Figure 2. Experimental  $1n$ - and  $3n$ - removal cross sections for  ${}^{197}\text{Au}$  [6] (scaled to 1 A GeV) in comparison with theoretical calculations [8] (solid curve: 'soft-spheres' calculation with the harmonic-oscillator model; dashed curve: same for perturbation theory; dotted curve: 'sharp-cutoff' calculation with the harmonic-oscillator model using the parametrization of  $b_{min}$  from [18]).

sections with several approximations. The dotted line shows the 'sharp-cutoff' approximation with the parametrization of  $b_{min}$  from Benesh et al. [18], derived from Glauber calculations. While there is good agreement for the  $1n$  channel, the  $3n$  cross sections, which are dominated by DGDR excitation, are underestimated. Also shown in Fig. 2 (solid line) is the result of a calculation taking into account the transparency of the nuclei in near-grazing collisions with a Glauber-type ansatz using realistic (droplet-model) neutron and proton density distributions ('soft spheres model') [8], which leads almost to

the same results. This is particular true for the  $3n$  channel, and thus for the DGDR cross section, where a much stronger influence of the cut-off is expected. The dashed curve in Fig. 2 denotes a soft-spheres calculation using perturbation theory, which overestimates the  $1n$  cross sections considerably. Since in this calculation an arbitrary choice of  $b_{\min}$  is avoided it can be concluded that the harmonic oscillator model, with the population of the multi-phonon states given by Poisson statistics, is appropriate for the case of large- $Z$  systems. For comparison of the theory with the uranium data, the ‘sharp-cutoff’ model with  $b_{\min}$  from [18] in the harmonic approximation will be used.

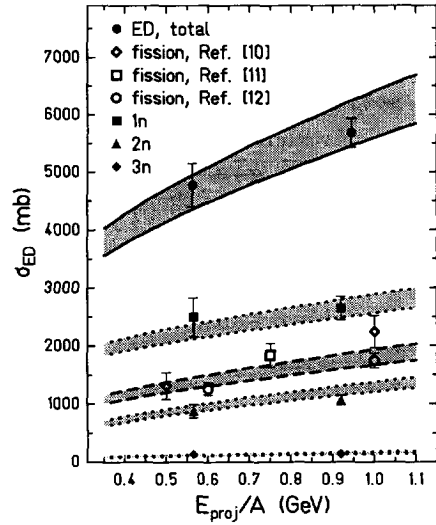
To obtain the cross sections for the ED of  $^{238}\text{U}$  also the fission deexcitation channel has to be taken into account in addition to the neutron-removal channels. Experimentally, photonuclear  $(\gamma, n)$  and  $(\gamma, f)$  cross sections have been measured with real photons up to about 18 MeV excitation energy [14,15]. For higher excitation energies the fission probability was extrapolated using known  $\Gamma_n/\Gamma_f$ -values [13]. The resulting  $xn$  cross sections are shown in Fig. 1 separately for the different contributions from the GDR (dashed curve) and the GQR (dotted curve), while the dot-dashed curve indicates the part of the cross section originating from DGDR excitation. It can be seen that the  $3n$  channel is clearly dominated by DGDR excitation. The total cross sections are obtained by summing up the different contributions and are shown in Fig. 1 for two input parameter sets for the GDR [14,15] (solid curves). The hatched area indicates this uncertainty in the calculation.

#### 4. COMPARISON BETWEEN THEORY AND EXPERIMENT

Fig. 2 shows that the  $1n$ -removal cross sections for  $^{197}\text{Au}$  targets (where fission decay after ED could be completely neglected) can be almost quantitatively reproduced even for large- $Z$  projectiles. As can be seen from Fig. 1 for the fissile projectile  $^{238}\text{U}$ , similar good agreement for the  $1n$  and  $2n$  channels can be found at both incident energies of 600 and 950 A MeV, respectively. Because of the lower  $2n$  threshold for  $^{238}\text{U}$  compared to  $^{197}\text{Au}$  not only the  $1n$  channel, but also the  $2n$  cross sections are dominated by single GDR excitation, as can be seen from Fig. 1. This indicates that the additional degree of freedom of the fission decay channel is correctly taken into account for  $^{238}\text{U}$ . An independent corroboration of this fact comes from direct experimental studies of the fission process (which is complementary to neutron emission) (Refs. [10–12]). These authors have determined cross sections for Coulomb fission of  $^{238}\text{U}$ . In Fig. 3 the ED cross sections for  $^{238}\text{U}+^{208}\text{Pb}$  are shown for the different  $xn$  and fission decay channels. The calculated cross sections are indicated by two curves for each channel, representing the two choices of GDR parameters. Also for the fission cross sections there is reasonably agreement between theory and experiment. From a comparison with the total ED cross sections one may conclude that the agreement is somewhat better if the GDR parameters of Veyssière et al. [14] (lower curve) are used.

From the decomposition of the individual contributions to the  $xn$  cross sections it is obvious that the dominant contribution to the  $3n$  cross section for the Pb target is the DGDR. All other processes increase much too slowly with target charge to come even close to the measured data point for the Pb target. When we compare our experimental  $3n$  cross sections with the results of our simple calculations, we find that also the  $3n$  channels show a similarly good agreement between experiment and theory as the (GDR-

Figure 3. Cross section for electromagnetic dissociation of  $^{238}\text{U}$ . The Coulomb fission cross sections from Ref. [10] are measured with  $^{208}\text{Pb}$  beams on  $^{238}\text{U}$ -targets, whereas the values from Ref. [11,12], as well as the  $xn$  cross sections from this work are obtained in inverse kinematics with  $^{238}\text{U}$ -beams. The data from Ref. [12], taken with Au-targets, were scaled to Pb. The curves indicate our theoretical calculations using two sets of experimental GDR parameters as an input.



dominated)  $1n$  and  $2n$  channels. This is in contrast with our previous investigation of  $3n$  removal from  $^{197}\text{Au}$  [6,8], where we encountered e.g. an excess of about 30 % for the system  $^{209}\text{Bi} + ^{197}\text{Au}$  (see Fig. 2).

Our calculation of the DGDR cross section involves a folding of the GDR with itself, implying that the DGDR has exactly twice the energy of the GDR and twice the width. Exclusive measurements have found evidence that the position of the DGDR is rather about 1.9 times the energy of the GDR, and about 20 % narrower than this simple estimate [2]. When we perform our calculation with these modifications, it turns out that they cancel each other almost quantitatively. Taken separately, a shift of the centroid by -1.2 MeV reduces the  $3n$  cross section by about 9 mb, whereas a reduction of the width by 20 % alone increases it by about 13 mb. An increase of the width would be required to take strength out of the  $3n$  channel. We cannot rule out, however, the possibility of an accidental compensation of a larger DGDR excitation probability and a larger fission probability. (It should be noted that e.g.  $3n$  emission occurs only in about one third of all cases with excitation energies in that range, whereas in the other two thirds the nucleus undergoes fission). Two recent experiments studying Coulomb fission of  $^{238}\text{U}$  (Refs. [11, 12]) have shown that the DGDR is also visible in the fission channel. By measuring the charge distribution of the fission fragments one can estimate the excitation energy of the fissioning system. The observed peak-to-valley ratio of about 7 [11,12] can only be explained if DGDR excitation is taken into account. Because of the uncertainties in this procedure it cannot be ruled out, however, that there is an excess of DGDR cross section in the fission channel.

As reported by J. Stroth [19] in his contribution to this conference, also for  $^{208}\text{Pb}$  a DGDR cross section was observed which is in agreement with the semiclassical calculation. The observed enhancement of DGDR cross sections in relativistic Coulomb excitation of Xe and Au seems no longer to be a general feature.

## 5. SUMMARY

By measuring formation cross sections of individually resolved isotopes of  $^{237-233}\text{U}$  at the GSI projectile-fragment separator, FRS, the electromagnetic dissociation of  $^{238}\text{U}$  could be studied as a function of target nuclear charge and bombarding energy. As in a previous study undertaken with  $^{197}\text{Au}$ , the  $1n$  channel has been found to be mainly sensitive to the GDR excitation, whereas the  $3n$  and  $4n$  channels are a sensitive probe of the DGDR excitation. In contrast to the  $^{197}\text{Au}$  case, we find no indication that a simple harmonic oscillator model of GDR excitation underestimates the  $3n$  cross section by any significant amount. It cannot be ruled out, however, that a larger-than-calculated DGDR cross section manifests itself only in the fission channel. The global trend, however, of electromagnetic neutron-emission and fission cross sections can be well described by our model.

## REFERENCES

1. FRS collaboration: H. Geissel, B. Blank, T. Brohm, H.-G. Clerc, S. Czajkowski, C. Donzau, A. Grewe, E. Hanelt, A. Heinz, H. Irnich, M. de Jong, A. Junghans, A. Magel, G. Münzenberg, F. Nickel, M. Pfützner, A. Piechaczek, C. Röhl, C. Scheidenberger, K.-H. Schmidt, W. Schwab, S. Steinhäuser, W. Trinder, and B. Voss.
2. H. Emling, Prog. Part. Nucl. Phys. **33**, 729 (1994).
3. Ph. Chomaz and N. Francaria, Phys. Rep. **252**, 275 (1995).
4. R. Schmidt et al., Phys. Rev. Lett. **70**, 1767 (1993).
5. J. Ritman et al., Phys. Rev. Lett. **70**, 533 (1993); *ibid.* **70** (1993) 2659.
6. T. Aumann et al., Phys. Rev. C **47**, 1728 (1993); Nucl. Phys. **A569**, 157c (1994) .
7. J.R. Beene, Nucl. Phys. **A569**, 163c (1994).
8. T. Aumann, C.A. Bertulani, and K. Sümmerer, Phys. Rev. C **51**, 416 (1995).
9. H. Geissel et al., Nucl. Instr. Meth. in Phys. Res. B **70**, 286 (1992).
10. S. Polikanov et al., Z. Phys. A **350**, 221 (1994).
11. P. Armbruster et al., submitted to Z. Phys. A.
12. Th. Rubehn et al., GSI Preprint, GSI-95-28 (1995).
13. T. Aumann et al., Z. Phys. A **352**, 163 (1995).
14. A. Veyssière et al., Nucl. Phys. **A199**, 45 (1973).
15. J.T. Caldwell et al., Phys. Rev. C **21**, 1215 (1980).
16. C.A. Bertulani and G. Baur, Phys. Reports **163**, 299 (1988).
17. W.J. Llope and P. Braun-Munzinger, Phys. Rev. C **41**, 2644 (1990); *ibid.* C **45**, 799 (1992).
18. C.J. Benesh, B.C. Cook, and J.P. Vary, Phys. Rev. C **40**, 1198 (1989).
19. J. Stroth et al., these proceedings.